Laminar–localized-phase coexistence in dynamical systems

G. Zumofen[1] and J. Klafter[2]
[1]*Laboratorium für Physikalische Chemie, Eidgenössische Technische Hochschule–Zentrum, CH-8092 Zürich, Switzerland*
[2]*School of Chemistry, Tel-Aviv University, Tel-Aviv, 69978 Israel*
(Received 23 February 1994)

A one-dimensional map is introduced which exhibits an intermittent chaotic behavior with coexisting laminar and localized phases. The generated trajectories demonstrate the interplay between the two competing motion modes and are analyzed in terms of Lévy statistics. The mean-squared displacements and the propagators of the motion are calculated and their relationship to an experimental realization is discussed.

PACS number(s): 05.40.+j, 05.45.+b, 03.20.+i, 47.52.+j

Anomalous diffusion in dynamical systems is by now well established [1–9]. One can observe in various dynamical systems dispersive [8] and enhanced [9] motions characterized by mean-square displacements that deviate from simple Brownian motion, namely, $\langle r^2(t)\rangle \sim t^{\alpha}$, with $\alpha > 1$ for motional enhancement and $\alpha < 1$ for the dispersive case. Both types of anomalies can be described theoretically by means of continuous-time random walks (CTRW) with broad distributions of trapping or flight times. In the latter case the common occurrence of Lévy statistics in dynamical systems has been demonstrated [5–7].

In a recent experiment by Solomon, Weeks, and Swinney [9] on tracer particles in a two-dimensional rotating flow, it has been observed that dispersive and enhanced modes of motion can coexist in such a way that a particle may perform long flights and be also intermittently trapped in space. Similar behavior has been observed by following trajectories in two-dimensional Hamiltonian systems, in the Chirikov-Taylor map, and in a model for surface diffusion [10]. The coexistence of laminar and localized modes has been addressed by Zaslavsky [11] using fractional Fokker-Planck equations.

In this paper we introduce a one-dimensional map that generates intermittent chaotic motion with coexisting dispersive and laminar motion events. This map is an extension of previously studied maps that lead either to dispersive or enhanced diffusion [2,5]. We demonstrate the applicability of the random walk scheme with Lévy stable-law distributions in analyzing the motion generated by the map. We show how the competing trends of laminar and localized phases lead to diffusional behavior, different than previously obtained, and cover the whole range of dispersive, regular, and enhanced behaviors. A related model applied to electrons in liquids has been discussed in Ref. [3].

Figure 1 shows the one-dimensional map which is defined as

$$f(x)=\begin{cases}(1+\epsilon)x+ax^{z}-1, & 0\le x\le \frac{1}{4}\\ (1+\tilde{\epsilon})x-\tilde{a}(\frac{1}{2}-x)^{\tilde{z}}, & \frac{1}{4}\le x\le \frac{1}{2}.\end{cases} \tag{1}$$

This (dissipative) map is discontinuous at the boundaries of each box but is continuous otherwise. For $\epsilon=\tilde{\epsilon}=0$ it shows marginal stable fixed points at $x=0$ and $x=\frac{1}{2}$. The neighborhood of the fixed point at $x=0$ is responsible for the laminarity, while the fixed point at $x=\frac{1}{2}$ gives rise to spatial localization. The exponents z and $\tilde{z}$ determine the characteristic behaviors of the two types of motion events, free flight and localized, respectively. The prefactors a and $\tilde{a}$ are just weights and are chosen so that the map function is continuous including the first derivative at $x=\frac{1}{4}$. For $\epsilon=\tilde{\epsilon}=0$ we used $a=4^{z}z/(z+\tilde{z})$ and $\tilde{a}=4^{\tilde{z}}z/(z+\tilde{z})$. ϵ and $\tilde{\epsilon}$ were considered to be small quantities and to differ from zero in the cases $z>2$ and $\tilde{z}>2$, respectively, in order to avoid problems in the numerical realization of the statistical analyses. This relatively simple map displays a rich spectrum of behaviors and a unique interplay of the two modes of motion.

In Fig. 2 we present two typical trajectories generated by the map defined in Eq. (1). The interplay of laminar and spatial localization (no motion) behavior is evident. The corresponding distributions of flight (laminar) and

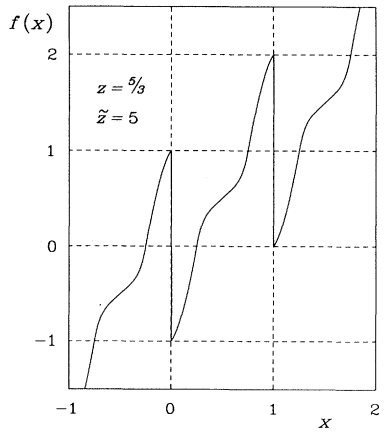

FIG. 1. The map $f(x)$ for the laminar-localized motion, Eq. (1), for $z=\frac{5}{3}$ and $\tilde{z}=5$, as indicated, corresponding to the exponents $\gamma=\frac{3}{2}$ and $\tilde{\gamma}=\frac{1}{4}$.

1063-651X/95/51(3)/1818(4)/$06.00

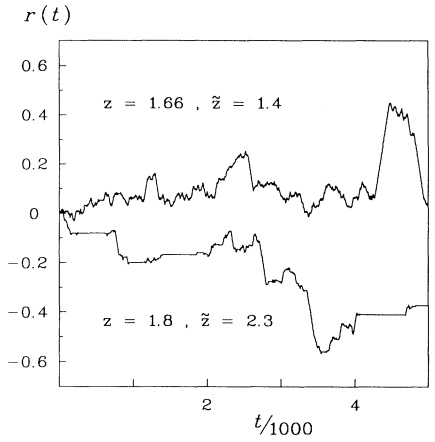

FIG. 2. Two typical trajectories. The upper curve for values $z=1.66$ and $\tilde{z}=1.4$, corresponding to $\gamma=1.5$ and $\tilde{\gamma}=2.5$, which give rise to enhanced diffusion with $\alpha=1.5$. The lower curve for values $z=1.8$ and $\tilde{z}=2.33$, corresponding to $\gamma=1.25$ and $\tilde{\gamma}=0.75$, which give rise to enhanced diffusion again with $\alpha=1.5$. Note that the localization phases and laminar phases occur on different scales.

localization times, as shown in Fig. 3, follow approximately power laws. For the laminarity and for the localization times we observe

$$\psi(t)\sim t^{-\gamma-1} \text{ and } \tilde{\psi}(t)\sim t^{-\tilde{\gamma}-1} , \tag{2}$$

respectively, with the exponents $\gamma=(z-1)^{-1}$ and $\tilde{\gamma}=(\tilde{z}-1)^{-1}$. The observed trajectories and the coexistence of the two motional modes resemble the behavior, although in a completely different type of system, that has been reported by Solomon, Weeks, and Swinney [9]. In this respect our map generates statistical properties that are amenable to experimental observation. What relates the different cases are the underlying Lévy stochastic processes, which we now outline.

We choose the velocity picture in which the particle moves continuously at a constant velocity, changes directions at random, and is occasionally interrupted by phases of spatial localization. This means that the particle does not move at a constant velocity at all times but that the phases of laminar motion are intermittently interrupted by periods of no motion on the scale of typically one box. The probability distribution to move a distance r in time t in a single motion event, in the laminar phase, and to stop at r for initiating a new motion event at random, is [5]

$$\psi(r,t)=\tfrac{1}{2}\delta(|r|-t)\psi(t) , \tag{3}$$

where length and time are given in dimensionless units. $\psi(t)$ is given in Eq. (2). Equation (3) defines the basic motion events in Lévy walks [5–7]. We further introduce $\Psi(r,t)$, the probability density to move a distance r in time t in a single motion event and not necessarily stop at r [5]:

$$\Psi(r,t)=\tfrac{1}{2}\delta(|r|-t)\int_t^\infty \psi(\tau)\,d\tau . \tag{4}$$

$\psi(r,t)$ and $\Psi(r,t)$ are the relevant quantities for the description of the laminar phase of the motion. For the localized case we note that

$$\tilde{\Psi}(t)=\int_t^\infty \tilde{\psi}(\tau)\,d\tau \tag{5}$$

is the probability for not having moved until time t. In the description of the propagator, the probability density to be at location r at time t, we assume that the observation starts with an event of motion at constant velocity and we can thus write

$$\begin{aligned}P(r,t)=\Psi(r,t)&+\int_0^t \psi(r,t')\tilde{\Psi}(t-t')\,dt' \\ &+\int_{-\infty}^{\infty} dr'\int_0^\infty dt'\int_0^{t'} dt''\psi(r',t'') \\ &\qquad\times\tilde{\psi}(t'-t'')\Psi(r-r',t-t') \\ &+\cdots ,\end{aligned} \tag{6}$$

where the first term denotes the probability to reach location r in time t in a single motion event. The second term is the probability to reach r at an earlier time and to stay localized until time t. The third term is the probability to reach r in time t in two motion events interrupted by one period of localization. The sum has to be extended over all possible combinations of motion events interrupted by periods of localization. Taking the Fourier-Laplace transform and summing over even and odd terms independently we obtain

$$P(k,u)=\frac{\Psi(k,u)+\tilde{\Psi}(u)\psi(k,u)}{1-\tilde{\psi}(u)\psi(k,u)} . \tag{7}$$

Here and in what follows we make use of the convention that the variables denote in which space (Fourier and/or Laplace) the function is thought to hold. A similar expression is obtained when the walks are initiated by a localization event followed by motion at constant velocity. Furthermore, for the analysis of iterated maps in terms of CTRWs we have demonstrated that stationary conditions are an important issue [10].

For the derivation of the mean-squared displacement we make use of $\langle r^2(t)\rangle=\mathcal{L}^{-1}\{-\partial_k^2 P(k,u)|_{k=0}\}$. From

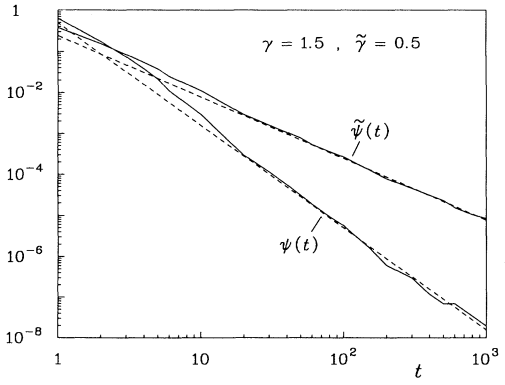

FIG. 3. The probability distributions $\psi(t)$ and $\tilde{\psi}(t)$ for $\gamma=1.5$ and $\tilde{\gamma}=0.5$, as indicated. Simulation results are given by solid lines; the dashed lines indicate the power laws of Eq. (2).

an analysis of the asymptotic behavior we derive the leading term for the mean-squared displacement $\langle r^2(t)\rangle \sim t^{\alpha}$, with the exponent α depending on γ and $\tilde{\gamma}$, namely,

$$\alpha = \begin{cases} 2+\min\{\tilde{\gamma},1\}-\min\{2,\gamma\}, & \gamma>1 \\ 2+\min\{\tilde{\gamma},\gamma\}-\gamma, & 0<\gamma<1. \end{cases} \tag{8}$$

In our simulation calculations we have concentrated on the regime $1<\gamma<2$, which corresponds to the intermediate enhanced diffusion regime if localization is disregarded [5]. According to Eq. (8) the combined effects lead to the mean-squared displacement

$$\langle r^2(t)\rangle \sim \begin{cases} t^{2+\tilde{\gamma}-\gamma}, & 1<\gamma<2, \quad \tilde{\gamma}<1 \\ t^{3-\gamma}, & 1<\gamma<2, \quad \tilde{\gamma}>1. \end{cases} \tag{9}$$

Equation (9) indicates that, depending on the two exponents γ and $\tilde{\gamma}$, the motion shows enhanced, regular, or dispersive behavior. It should be noted that for $\tilde{\gamma}>1$, for which $\tilde{\psi}(t)$ in Eq. (2) has a finite first moment, the enhancement reduces to the result obtained by the original Lévy-walk scheme [5,12]. In Ref. [9] the exponents $\mu=2.3\pm0.2$ for the flights, $\nu=1.6\pm0.3$ for the sticking, and $\alpha=1.65\pm0.15$ for the mean-squared displacement are reported, which were determined from independent measurements. According to the convention of Eq. (2) we have $\gamma=\mu-1=1.3\pm0.2$ and $\tilde{\gamma}=\nu-1=0.6\pm0.3$ so that we obtain from Eq. (8) $\alpha=1.3\pm0.5$, which is consistent with the experimental value.

In Fig. 4 we show numerical results for the time evolution of the displacements. Plotted is the ratio $\langle r^2(t)\rangle/t$ for various γ and $\tilde{\gamma}$ values. The denominator t has been chosen to strengthen the impression of the deviation from simple Brownian motion. The results follow reasonably the predicted power-law behaviors. Different time exponents are found for $\langle |r(t)|\rangle^2$, which may even display dispersions ($\alpha<1$) when $\langle r^2(t)\rangle$ is enhanced ($\alpha>1$), e.g., for $\gamma=1.25$ and $\tilde{\gamma}=0.5$.

For the intermediate-enhanced diffusion regime, $1<\gamma<2$, relevant to the behavior discussed in this paper, and $\tilde{\gamma}>1$, the small (k,u) expansion of the propagator gives up to the leading terms $P(k,u)\sim(u+c|k|^{\gamma})^{-1}$, which yields the known Lévy stable distribution [5]

$$P(r,t)\sim \begin{cases} t^{-1/\gamma}L_{\gamma}(\xi), & r<t \\ 0, & r>t, \end{cases} \tag{10}$$

where ξ is the scaling variable $\xi=cr/t^{1/\gamma}$ and the cutoff is due to the δ-function correlation in Eq. (3). Here the laminar phase dominates the transport properties.

A different behavior is derived for $1<\gamma<2$ and $\tilde{\gamma}<1$, where the small (k,u) expansion of the propagator gives $P(k,u)\sim u^{\tilde{\gamma}-1}(u^{\tilde{\gamma}}+c|k|^{\gamma})^{-1}$. This leads to the approximate scaling form

$$P(r,t)\sim \begin{cases} t^{-\tilde{\gamma}/\gamma}Q(\xi), & \xi\to 0 \\ t^{-\tilde{\gamma}/\gamma}\xi^{-\gamma-1}, & r\to t \\ 0, & r>t, \end{cases} \tag{11}$$

where $Q(\xi)$ is a scaling function. Depending on γ and $\tilde{\gamma}$, $Q(\xi)$ shows a cusp at the origin [10]. The scaling variable is $\xi=r/t^{\tilde{\gamma}/\gamma}$. In the case of $\gamma>2$ and $\tilde{\gamma}<1$ we recover the dispersive behavior treated in Ref. [5]. Here the role of localization is pronounced and may even dominate, a situation which we did not observe in Hamiltonian systems [10]. From the scaling in Eqs. (10) and (11) we notice that for the average of the absolute value of the displacement we have $\langle |r(t)|\rangle \sim t^{\min(1,\tilde{\gamma})/\gamma}$ for $1<\gamma<2$, in agreement with the results in Ref. [11].

Finally, in Fig. 5 we give the results for the propagator for $\gamma=\tilde{\gamma}=1.25$ in the scaling representation. Because of the finite mean trapping time the propagator, as expected, follows the stable law, Eq. (10), for $r<t$. The collapse of the lines for various times onto a single master curve indicates that scaling holds. The peaks at $r=0$ and $r=t$ are attributed to stationary condition effects which result from the method of averaging [5,13].

Summarizing, we have introduced a one-dimensional map that exemplifies the coexistence of free flights and

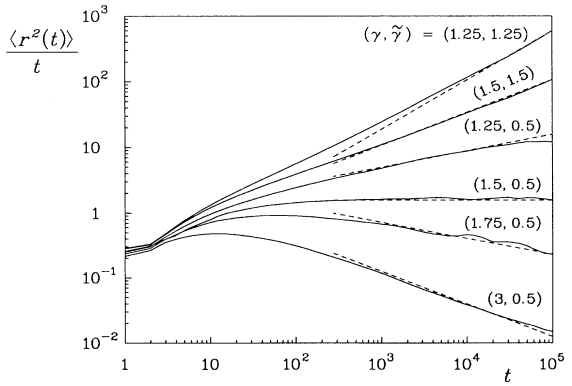

FIG. 4. The time evolution of the mean-squared displacement for various enhanced and dispersive cases. The numerical results of $\langle r^2(t)\rangle/t$ are given by solid lines for γ and $\tilde{\gamma}$ values as indicated. The dashed lines are the predicted slopes according to Eq. (9).

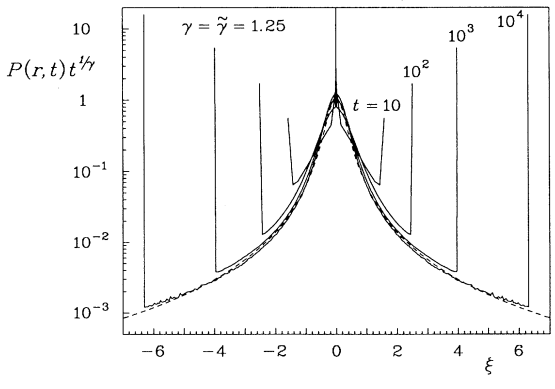

FIG. 5. The propagator $P(r,t)$ for $\gamma=\tilde{\gamma}=1.25$. The numerical results are plotted as solid lines for times t, as indicated, in the scaling representation with the scaling variable $\xi=r/t^{1/\gamma}$. The dashed line is the stable law $cL_{\gamma}(cx)$ with c adjusted to the map parameters.

spatial traps. The resulting intermittent laminar-localized motion has been analyzed in terms of CTRWs and Lévy statistics and the predictions have been corroborated by numerical calculations. We have shown that, depending on the two exponents γ and $\tilde{\gamma}$, the asymptotic behavior is dominated by the localized-dispersive or laminar-enhanced type of motion.

We are grateful to Professor K. Dressler for helpful discussions and to F. Weber for technical assistance. J.K. thanks the ETH for hospitality during the time this work was carried out. A grant of computer time from the Rechenzentrum der ETH-Zürich is gratefully acknowledged.

[1] C. F. F. Karney, Physics D **8**, 360 (1983).
[2] T. Geisel, J. Nierwetberg, and A. Zacherl, Phys. Rev. Lett. **54**, 616 (1985); T. Geisel and S. Thomae, *ibid.* **52**, 1936 (1984); T. Geisel, A. Zacherl, and G. Radons, *ibid.* **59**, 2503 (1987).
[3] M. F. Shlesinger and J. Klafter, J. Phys. Chem. **93**, 7023 (1989).
[4] A. A. Chernikov, B. A. Petrovichev, A. V. Rogalsky, R. Z. Sagdeev, and G. M. Zaslavsky, Phys. Lett. A **144**, 127 (1990); D. K. Chaikovsky and G. M. Zaslavsky, Chaos **1**, 463 (1991).
[5] G. Zumofen and J. Klafter, Phys. Rev. E **47**, 851 (1993); G. Zumofen, J. Klafter, and A. Blumen, *ibid.* **47**, 2183 (1993).
[6] M. F. Shlesigner, G. M. Zaslavsky, and J. Klafter, Nature **263**, 31 (1993).
[7] G. Zumofen and J. Klafter, Europhys. Lett. **25**, 565 (1994).
[8] O. Cardoso and P. Tabeling, Europhys. Lett. **7**, 225 (1988).
[9] T. H. Solomon, E. R. Weeks, and H. L. Swinney, Phys. Rev. Lett. **71**, 3975 (1993).
[10] J. Klafter and G. Zumofen, Phys. Rev. E **49**, 4873 (1994).
[11] G. M. Zaslavsky, Chaos **4**, 1 (1994); G. M. Zaslavsky, D. Stevens, and H. Weitzner, Phys. Rev. E **48**, 1683 (1993).
[12] M. F. Shlesinger, B. J. West, and J. Klafter, Phys. Rev. Lett. **58**, 1100 (1987); J. Klafter, A. Blumen, and M. F. Shlesinger, Phys. Rev. A **35**, 3081 (1987).
[13] J. Klafter and G. Zumofen, Physica A **196**, 102 (1993).